Available online at www.sciencedirect.com

SciVerse ScienceDirect

Physics Procedia 37 (2012) 72 – 78

Physics Procedia

TIPP 2011 - Technology and Instrumentation for Particle Physics 2011

Upgrade of the CMS Hadron Outer Calorimeter with SIPMs

Jacob Anderson*, James Freeman, Sergey Los, Juliana Whitmore
for the CMS HCAL Collaboration

Fermi National Accelerator Laboratory, Batavia, IL 60510, USA

Abstract

The CMS Hadron Outer Calorimeter (HO) is undergoing an upgrade to replace the existing hybrid photodetectors (HPDs) with silicon photo-multipliers (SIPMs). The chosen device is the Hamamatsu $3 \times 3\,\text{mm}^2$ $50\,\mu\text{m}$ pitch MPPC. The system has been developed to be a "drop-in" replacement of the HPDs. A complete control system of bias voltage generation, leakage current monitoring, temperature monitoring, and temperature control using solid state Peltier coolers has been developed and tested. 108 channels of the system have been installed into CMS and operated for more than 2 years. The complete system of about 2200 channels is in production and will be installed in the next LHC long shut-down scheduled for 2013.

Keywords: SIPM, CMS, Calorimeter, Hadron

1. Overview

The CMS central calorimeter consists of a detector inside the solenoidal magnet, HB, and a component outside the magnet, the Outer Hadron Calorimeter, HO [1]. The HO is installed inside the magnet flux return yoke and provides for typically 3λ of additional absorber to the calorimetric measurement. The outer calorimeter is composed of one or two 1 cm layers of BC408 scintillator with 0.94 mm diameter wavelength shifting fiber readout into photodetectors. Fig. 1a shows the schematic layout of the calorimeters in CMS and shows the location of the HO scintillator layers. The front end electronics are placed inside the CMS detector, close to the scintillators. Fig. 1b shows a photograph of the scintillators. Note the four wavelength shifting fibers per tile. The tile size creates a projective tower with the HB. Currently the photodetector used is the HPD [2] but for performance and operational reasons it is desired to upgrade these with SIPMs.

The CMS HCAL group has developed a drop-in replacement for the HPD using SIPMs [3, 4]. SIPMs are very suitable for this application because of several factors: The radiation levels are modest with a lifetime expected fluence of less than 5×10^{11} neutrons/cm^2 (E $>$ 100 KeV). The energy flux into HO is small, the rate of larger energy depositions is low, and the required dynamic range is modest. The HO is in

*corresponding author
Email address: andersj@fnal.gov (Jacob Anderson)

1875-3892 © 2012 Published by Elsevier B.V. Selection and/or peer review under responsibility of the organizing committee for TIPP 11.
Open access under CC BY-NC-ND license. doi:10.1016/j.phpro.2012.02.358

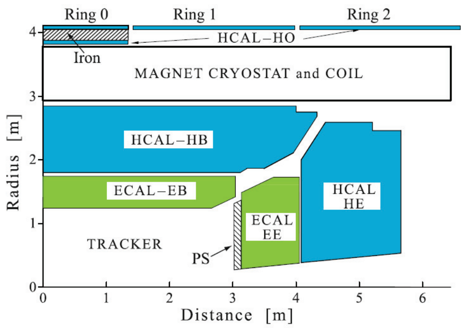

(a) Diagram of quarter section of CMS showing the location of the HCAL components. The HO is located in the iron rings of the return yoke immediately outside of the solenoid.

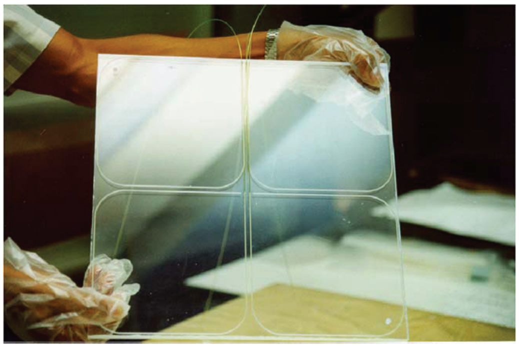

(b) An HO scintillator tile

Fig. 1: The CMS outer hadron calorimeter

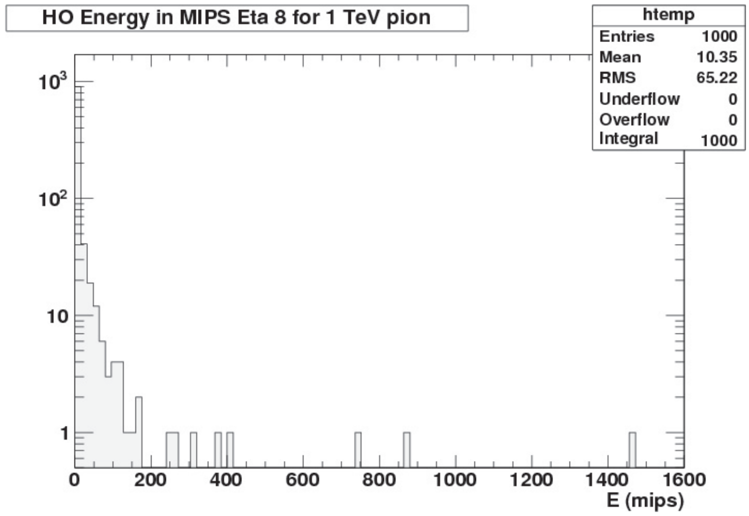

Fig. 2: Energy deposition in MIPs into HO for 1000 GeV pions. One MIP corresponds to about 12 pes.

the return magnetic field of up to 2 kG and the photodetector needs to operate in that environment. Finally, the available physical volume for the photodetectors is small.

2. SIPM choice

Fig. 2 shows the energy deposition into HO for simulated 1000 GeV pions. We note that the distribution does not have substantial population above 200 MIPs. Studies show that the correlation between incident energy and energy deposited into HO is lost at large energy depositions into HO. For these reasons we chose 200 MIPs as the required dynamic range. With 12 photoelectrons (pe) per MIP, this corresponds to about 2500 pes.

We had a number of constraints/features of the SIPM we needed to emphasize. Important requirements were:

- Rad. tolerance to 5×10^{11} neutrons (> 100 KeV)/cm^2
- Dynamic range sufficient for HO (2500 pes)

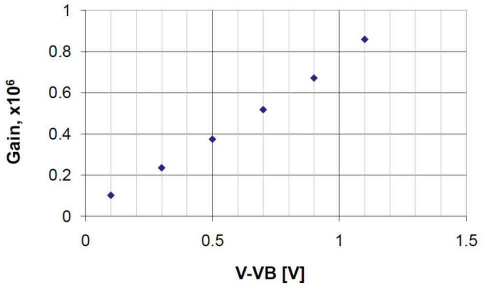

(a) Gain as a function of applied over-voltage.

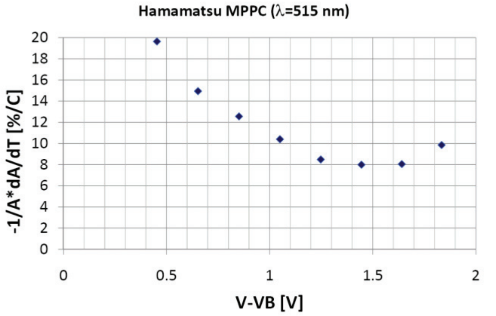

(b) Temperature dependence of gain as a function of over-voltage.

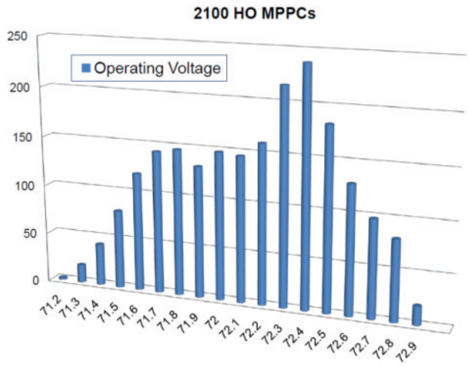

(c) Variation in operating voltage for 2100 MPPCs

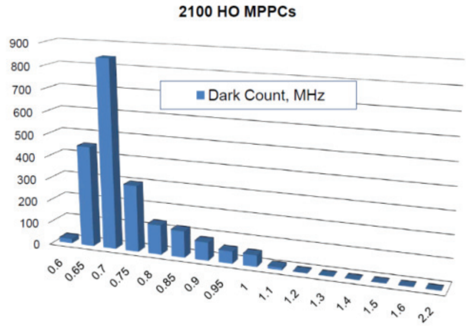

(d) Variation in dark count for 2100 MPPCs

Fig. 3: MPPC charateristics

- Pulse recovery time ($\tau \approx 25$ ns)
- Low leakage current
- Photon detection efficiency ($\approx 25\%$)
- Temperature dependence of gain (few % per degree C)
- Low source capacitance
- Match to the spectral response from the wavelength shifting fiber (500 nm)

We performed an evaluation [5, 6] of different SIPM candidates and decided that the Hamamatsu $3 \times 3\,\text{mm}^2$ 50 μm pitch MPPC was the appropriate choice of SIPM. We have ordered and received about 3000 of these devices. These devices have 3600 micro-pixels which is a good match for our required dynamic range. At the wavelength of interest, 500 nm, the MPPC has a PDE (photon detection efficiency) of 25%–30%. The capacitance of the MPPC (at operating voltage) is about 300 pF. As seen in Fig. 3a, the gain of the MPPC is about 6×10^5 at 1 volt over-voltage. For 2500 pes, this corresponds to 250K fC of charge. The MPPC pulse width for our signal is roughly 50 ns.

Fig. 3b shows the temperature dependence of the MPPC gain as a function of over-voltage for a fixed operating voltage. It is large, with a minimum of 8%/°C at 1.5 volts over-voltage. The large temperature dependence forces the need to actively control the temperature of the SIPM location.

Figs. 3c and 3d show properties of 2100 MPPCs of the total order of 2900. Fig. 3c is the variation in operating voltage for a gain of 7.5×10^5, and Fig. 3d is the dark count in MHz at the operating voltage and 25° C.

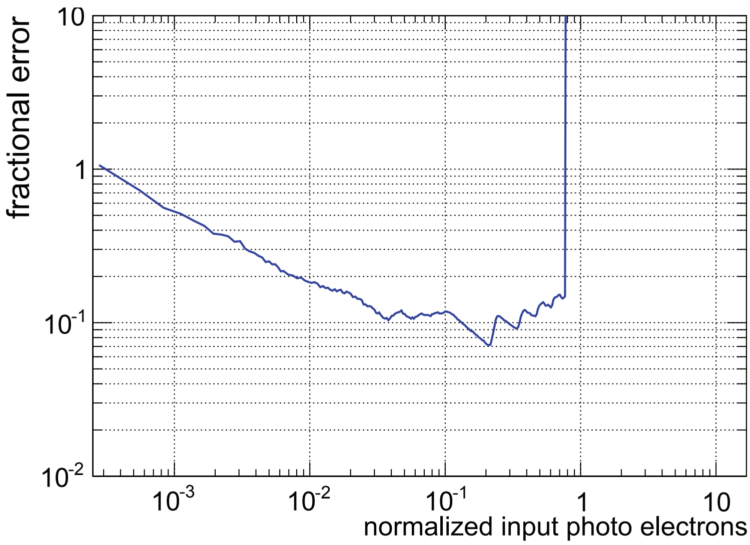

Fig. 4: Fractional error (simulated) for the digitized QIE8 signal as a function of number of pes per MPPC micro-pixel. The sharp verticle line is where the QIE8 ADC saturates.

3. System design

The original HPD was built in one unit with 18 individual readouts. The drop-in replacement is required to match that physical layout. The photodetector and front end electronics are housed in crates (RBX) that are installed inside the magnet return yoke. Electronics and photodetectors are arranged into independent Readout Modules (RMs) inside the RBX.

The drop-in system had to supply a self-contained operating environment for the SIPM. The SIPM has a large temperature dependence of the gain. We needed local temperature stabilization to better than 0.1° C. Temperature is stabilized using a Peltier cooler. About 1 watt of power can be removed per RM and a δ(T) of approximately 10° C can be achieved.

The system has:

- Local temperature sensing and stabilization (Peltier and software feedback correction voltage)
- Hardware under-temperature protection
- Leakage current measurement
- Bias voltage generation (CW from LV volt supply)

The SIPM is AC coupled to the 40 MHz flash front end ADC (QIE version 8) [7, 8] through a 22 nF capacitor. The coupling network achieves signal charge attenuation through capacitive splitting with the resulting gain of 50,000. This corresponds to about 20K fC, split approximately into 1/2 in one 25 ns sample, and the remaining 1/2 split into 2 trailing samples. The maximum charge measurement for the QIE8 is 10K fC which matches the attenuated maximum anticipated signal of 200 MIPs.

Fig. 4 shows the simulated performance of the MPPC/QIE8 for the nominal gain. The figure shows fractional quantization error as a function of pes per MPPC micro-pixel. There are 3600 micro-pixels in the MPPC so the value “1” in the plot corresponds to 3600 incident pes. The QIE8 digitization granularity is shown as the stair-stepping. Note that we achieve an acceptable fractional error of 10% even in the case where we approach one pe (on the average) per micro-pixel.

The SIPM bias voltage (BV) is generated locally from 6.5 V LV using a Cockcroft-Walton. 18 independent channels can regulate from 0 V to 100 V and supply 100 μA per channel. The BV is settable with a least count of 25 mV and is stable to about 5 mV. The SIPM leakage current can be read back for each channel, with a precision of 10 nA. Table 1 shows some of the system parameters.

Table 1: Control Board Parameters

Control board parameter	
Bias Voltage Range	0–100 V
BV Setting Resolution, LSB	25 mV
Hardware Current Limit (per channel)	100 μA
Leakage Current Full Scale	40 μA
Leakage Current Resolution, LSB	10 nA
Temperature Resolution, LSB	0.018° C

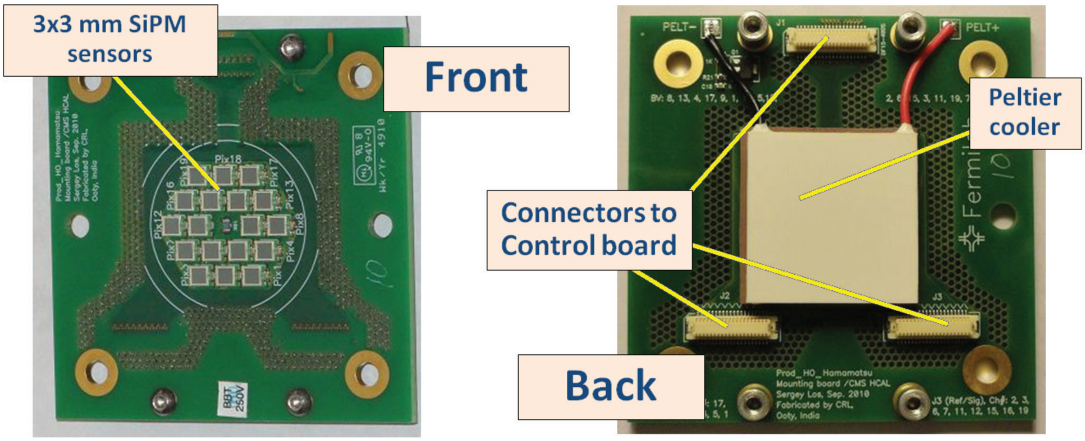

Fig. 5: Photographs of the two sides of the Mounting Board (MB).

The SIPM system developed consists of 2 circuit boards, the Mounting Board (MB) and the Control Board (CB). The array of 18 SIPMs is mounted on one side of the MB. On the other side a Peltier cooler is placed to arrange for a constant temperature of the SIPM. Both sides of the MB are shown in Fig. 5. Fig. 6 shows details of the placement of the CB and MB in the RM unit of the RBX. To set the scale, the CB and MB are about 6.5 cm × 6.5 cm.

In Fig. 5 note the perforations around the SIPM area on the MB to provide for thermal isolation. The temperature of the SIPM area is read out using a precision platinum resistor. The CMS slow control system reads out the temperature and generates a correction voltage to apply to the Peltier cooler. The control loop is execute about once per minute. Fig. 7 shows a typical measurement of temperature vs time for the SIPM area. The least count of the readout is 0.018° C. We see that the temperature is stable to about 1 least count over a period of hours. The peaks in in Fig. 7 are two transient temperature excursions introduced to demonstrate the temperature settling time. A hardware protection circuit is set to prevent the Peltier from driving the temperature below the dew point. The trip temperature is 15° C.

In order to ensure uniform illumination of the $3 \times 3\,\text{mm}^2$ SIPM surface, we employ a light mixer of a few millimeters thickness. These are constructed as thin discs with either 3 mm diameter fiber insets. These mixers prevent local SIPM saturation from light coming from only one of the fibers from the scintillator tiles.

4. Performance

108 SIPMs have been installed and operated in CMS for about 2 years. They have proven to be reliable and well-functioning. Noise observed for channels using HPDs have not been seen in the SIPMs. The MIP

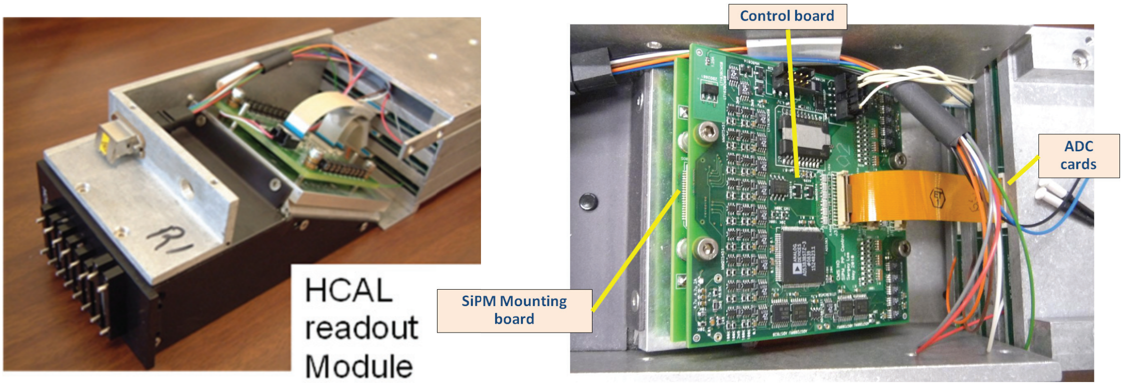

Fig. 6: Views of an opened RM where the Control Board (CB) is seen. In the left photo note the connection to the ADC cards (QIEs).

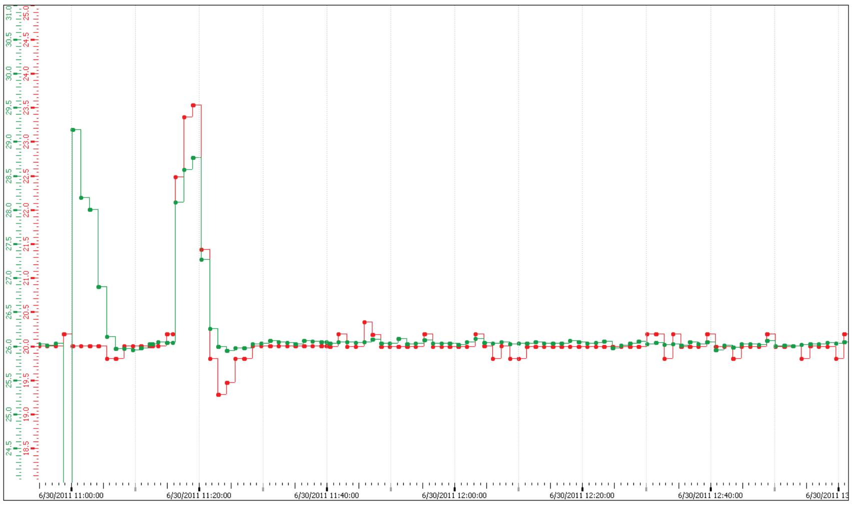

Fig. 7: Temperature measurement of the SIPM area vs time (Green curve). The horizontal axis shows a two hour period. The peaks in the traces are temperature excursions introduced to show the settling time of the feedback.

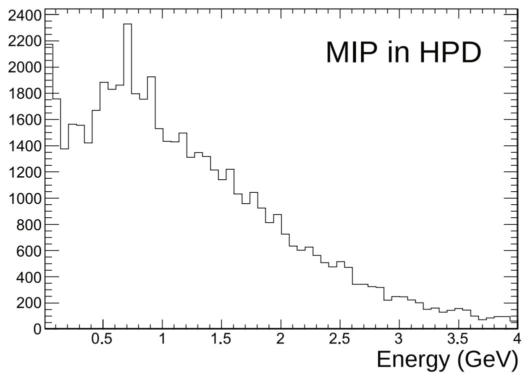

(a) HO MIP signal from HPD channel

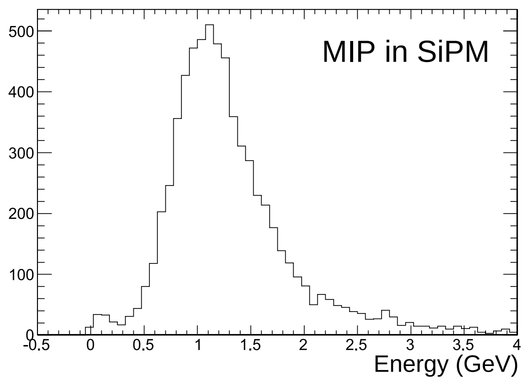

(b) HO MIP signal from SIPM channel

Fig. 8: MIP performance of the HO.

signal can be clearly measured with the SIPMs. Fig. 8a shows a typical observed HPD MIP signal and Fig. 8b shows a MIP signal from the SIPM. The signal to noise for a MIP in HO for the SIPM is seen to be about 20:1.

5. Schedule

The MB and CB boards are currently in production. During the next LHC shut-down (scheduled for February 2012) 100 or more channels of the new system will be installed. At the following LHC long shut-down, 2013, the remainder of the system will be installed.

References

[1] S. Abdullin, et al., Design, performance, and calibration of the CMS Hadron-outer calorimeter, Eur.Phys.J. C57 (2008) 653–663. doi:10.1140/epjc/s10052-008-0756-6.

[2] P. Cushman, A. Heering, CMS HCAL hybrid photodiode design and quality assurance stations, ICFA Instrum.Bull. 25 (2002) 1–16.

[3] J. Freeman, Silicon photomultipliers for the CMS Hadron Calorimeter, Nucl.Instrum.Meth. A617 (2010) 393–395. doi:10.1016/j.nima.2009.10.132.

[4] J. Freeman, Innovations for the CMS HCAL, Int.J.Mod.Phys. A25 (2010) 2421–2436. doi:10.1142/S0217751X10049682.

[5] A. Heering, J. Rohlf, J. Freeman, S. Los, S. Kuleshov, S. Banerjee, I. Schmidt, Y. Musienko, L. Lebolo, J. Diaz, Large-area SiPMs for the CMS hadron outer calorimeter, in: Nuclear Science Symposium Conference Record, 2007. NSS '07. IEEE, Vol. 2, 2007, pp. 1545 –1550. doi:10.1109/NSSMIC.2007.4437293.

[6] A. Heering, et al., Performance of silicon photomultiplers with the CMS HCAL front-end electronics, Nucl.Instrum.Meth. A576 (2007) 341–349. doi:10.1016/j.nima.2006.11.049.

[7] T. Shaw, A. Baumbaugh, A. Boubekeur, J. Elias, J. Hoff, S. Holm, S. Los, C. Rivetta, A. Ronzhin, J. Whitmore, T. Zimmerman, R. Yarema, Front end readout electronics for the CMS Hadron Calorimeter, in: Nuclear Science Symposium Conference Record, 2002 IEEE, Vol. 1, 2002, pp. 194 – 197 vol.1. doi:10.1109/NSSMIC.2002.1239297.

[8] T. Zimmerman, J. R. Hoff, The Design of a charge integrating, modified floating point ADC chip, IEEE J.Solid State Circuits 39 (2004) 895–905. doi:10.1109/JSSC.2004.827808.